WILEY | Hindawi

Research Article

Reactive Blue 2 Labels Protamine in Late-Haploid Spermatids and Spermatozoa and Can Be Used for Toxicity Evaluation

Satoshi Yokota [iD],[1] **Tomohiko Wakayama** [iD],[2] **Hidenobu Miyaso** [iD],[3] **Kousuke Suga** [iD],[1] **Masakatsu Fujinoki** [iD],[4] **Satoru Kaneko** [iD],[5] **and Satoshi Kitajima** [iD][1]

[1]*Division of Cellular & Molecular Toxicology, Center for Biological Safety & Research, National Institute of Health Sciences, 3-25-26 Tono-machi, Kawasaki-ku, Kawasaki, Kanagawa 210-9501, Japan*
[2]*Department of Histology, Graduate School of Medical Sciences, Kumamoto University, Honjo, Kumamoto, Japan*
[3]*Department of Anatomy, Faculty of Medicine, School of Medicine, International University of Health and Welfare, Narita, Chiba, Japan*
[4]*Research Lab of Laboratory Animals, Research Center for Laboratory Animals, Comprehensive Research Facilities for Advanced Medical Science, School of Medicine, Dokkyo Medical University, Tochigi, Japan*
[5]*Department of Obstetrics and Gynecology, Ichikawa General Hospital, Tokyo Dental College, Ichikawa, Chiba, Japan*

Correspondence should be addressed to Satoshi Yokota; s-yokota@nihs.go.jp

Reactive blue 2 (RB2) dye specifically binds to the nuclei of human spermatozoa under weakly alkaline conditions, thereby providing a new method for assessing sperm quality. However, this technique has not yet been applied to other mammalian species, such as well-established rodent models, which would allow evaluation of the male reproductive toxicity of new drug candidates in nonclinical studies. We aimed to evaluate the usefulness of RB2 staining in assessing testicular and epididymal sperm toxicity in mice using a busulfan-induced infertility model. Male C57BL/6J mice were intraperitoneally administered 40 mg/kg of busulfan. After 28 days, the testes and epididymis were collected and stained with RB2 at pH 10. In vitro evaluations were conducted on uncoated glass slides with RB2 mixed with mouse synthetic protamines, protamines extracted from the human spermatozoa or intracellular protein components from somatic cells without protamines. Following peanut agglutinin lectin histochemistry, RB2-positive cells were observed in elongating and elongated spermatids at all stages except for stages IX–XI of the seminiferous epithelium. After busulfan administration, the proportion of RB2-positive germ cells in the seminiferous tubules was significantly decreased, and no RB2-positive spermatozoa were found in the caput epididymis of treated mice. Aggregates were observed in a mixture of RB2 dye (pH 10) and protamines but not in a mixture of intracellular protein components without protamines, and this specificity was lost at a neutral pH. Our study demonstrated that RB2 specifically stains steps 12–16 spermatids, indicating specific binding to the protamines expressed in these spermatids. The RB2 staining technique has potential as a biomarker for male reproductive toxicity, allowing for the rapid visualization of protamination in an animal model commonly used for the evaluation of male reproductive toxicity.

1. Introduction

The International Council for Harmonisation of Technical Requirements for Pharmaceuticals for Human Use guidelines require histopathological evaluation of the effects of a candidate drug using hematoxylin and eosin (H&E) staining in nonclinical animal studies, including general toxicity studies as well as male reproductive toxicity studies [1]. Specifically, testicular toxicity must be evaluated prior to the first clinical trial in humans. If pharmaceutical candidates show potential testicular toxicity, nonclinical animal testing must be withdrawn. Although regulatory guidelines do not include specific recommendations for general toxicity studies using animals in the evaluation of male reproductive toxicity,

nonclinical testicular toxicity testing could be preferable for detecting changes that may occur in clinical trials. However, the results of nonclinical animal testing do not necessarily match the effects in humans [2, 3]. Furthermore, identification and interpretation of chemically induced changes in testis histology require a fundamental knowledge of spermatogenesis. However, no H&E-based staining technique is currently available for the specific identification of male germ cell development. Thus, a novel HE-based staining method for specific staining of spermatogenic cells is needed to support the interpretation of the results of histopathological analysis.

During the late haploid phase of spermatogenesis (spermiogenesis), mammalian spermatozoa undergo protamination, in which more than 90% of histones, which package DNA in early spermatids, are removed from the DNA and are replaced by transition nuclear proteins and finally by protamines (PRMs) [4]. PRMs possess more domains rich in arginine (Arg), a basic amino acid, than do histones and transition nuclear proteins. These domains promote sperm head condensation and DNA stabilization by binding to the phosphoric group in DNA [5]. The importance of PRMs in sperm chromatin condensation and the influence of protein expression on sperm function have been shown in both mouse and human studies [6–9]. In most mammals, sperm chromatin is packaged by a single PRM, whereas primates and most rodents, as well as a subset of other placental mammals, express two PRMs: protamine 1 (PRM1) and protamine 2 (PRM2). Alterations in the content of sperm PRMs induce negative effects on sperm concentration, motility, and sperm head morphology in men [8]. Haploinsufficiency of PRMs in mice results in sperm morphological abnormalities, DNA damage, and decreases in sperm motility [10]. In particular, PRM2-deficiency has a negative impact on chromatin packaging and sperm head morphology [7]. Incorrect condensation of sperm chromatin leads to sperm head abnormalities, such as larger heads [11]. These findings suggest that PRM levels could serve as a biomarker of male infertility [6].

A previous study showed that reactive blue 2 (RB2) (Figure S1) dye specifically binds to the nucleus of human spermatozoa under weakly alkaline conditions (pH 10), providing a new method for assessing human sperm quality [12]. At this weak basic pH, the three sulfate residues in RB2 may bind to the guanidyl groups in Arg through electrostatic interactions, enabling specific staining of PRMs in human spermatozoa [12]. It would be useful if RB2 staining could be applied in nonclinical studies for evaluating male reproductive toxicity in rodent models; however, this technique has not yet been attempted in mammalian species other than humans. Based on the chemical structure of RB2, we hypothesized that RB2 would also specifically bind to PRMs in the haploid germ cells of other male mammals under weakly alkaline conditions.

Therefore, the aim of the present study was to examine whether the germ cell specificity of RB2 observed in humans is consistent in experimental mammalian models, such as mice. Specifically, we investigated whether PRMs could be visualized using RB2. To this end, we performed an in vitro experiment to examine the usefulness of this staining technique for evaluating testicular and epididymal sperm toxicity using a standard mouse model of busulfan-induced infertility [13–16].

2. Materials and Methods

2.1. Animals. Twelve C57BL/6J male mice (CLEA Japan, Tokyo, Japan), aged 5 weeks, were maintained under standard laboratory conditions. The mice were housed (three mice per cage) in ventilated cage systems (Lab Product Inc., Seaford, DE, USA) at $23 \pm 2°C$ under a 12-hr light/dark cycle (lights on from 8:00 to 20:00), with *ad libitum* access to food and water. Body weight (21.46 ± 0.9 g) was measured once a week.

This study followed the guidelines established by the ethical committee for animal experiments of the National Institutes of Health Sciences (NIHS). The animal facility was approved by the Health Science Center for the Accreditation of Laboratory Animal Care in Japan. All experimental protocols in the study were reviewed and approved by the Committee for Proper Experimental Animal Use and Welfare, a peer-review panel established at the NIHS, under experimental approval no. 816.

2.2. Experimental Design. After a 1-week habituation period, 12 mice were randomly divided into two groups: the vehicle control group ($n = 6$) and the busulfan-treated group ($n = 6$). The vehicle control group received two intraperitoneal (i.p.) injections of vehicle (10% dimethyl sulfoxide (DMSO; 031-24051; CultureSure®DMSO; FUJIFILM Wako Pure Chemical Industries, Ltd., Osaka, Japan)) in saline (Otsuka Pharmaceutical Co., Tokyo, Japan) with a 3-hr interval between injections. Busulfan (B-2635; Sigma-Aldrich, St. Louis, MO, USA) was dissolved in DMSO at a concentration of 10 mg/mL and then gradually added to a $9 \times$ volume of saline (final concentration: 1 mg/mL). Similar to the vehicle control group, the busulfan-treated group received two i.p. injections (20 mL/kg per injection) of busulfan at a total dose of 40 mg/kg body weight, as previously described [13, 17]. After 28 days, the reproductive organs of the male mice were collected under 3.5% isoflurane anesthesia. All efforts were made to minimize animal suffering. Each mouse was weighed, blood was collected from the inferior vena cava, and the testes and epididymis were removed. Dissected tissues were fixed for histopathological analysis, as described below.

2.3. RB2 Staining of Spermatids in the Testes and of Spermatozoa in the Epididymis. For histopathological analysis, the testes and epididymis were removed and immersed in freshly prepared 4% paraformaldehyde phosphate buffer fixative (161-20141; FUJIFILM Wako Pure Chemical Industries, Ltd.) for 48 hr. Following fixation, the testes and epididymis were processed using a graded alcohol series, cleared in xylene, and embedded in paraffin. Sections (4-μm thick) were prepared, deparaffinized, and stained with H&E using our routine method, for overall morphological evaluation. Two serial testis sections were prepared: one was used for visualization of male germ cells expressing PRM

according to RB2 staining, and the other was applied for staging of the mouse seminiferous epithelium cycle using peanut agglutinin (PNA) lectin histochemistry, as previously described [18, 19].

For the former analysis, the testicular and epididymal cross-sections were stained with 0.1% RB2 (catalog no. 12236-82-7; RB2; R115; Sigma-Aldrich) in 100 mM carbonate–bicarbonate buffer (pH 10) for 30 min, and the excess dye was washed out with the carbonate–bicarbonate buffer. For the latter analysis, the sections were immersed in 20 mM Tris-HCl buffer (pH 9) and heated at 90°C for 30 min for antigen retrieval. After cooling to room temperature, the sections were washed in phosphate-buffered saline, incubated with Alexa Fluor 488-conjugated antilectin PNA antibody (L21409, 1 : 1,000; Molecular Probes, Eugene, OR, USA) for 30 min at room temperature to visualize the acrosomes, and then counterstained with Hoechst 33258 (Sigma-Aldrich). Each stage of spermatogenesis was determined to simplify the identification of the cell population, as previously reported [18, 19]. Briefly, testis sections from the control mice were observed to determine the staging of the seminiferous epithelium cycle. The 12 stages (I–XII) of spermatogenesis in mice were determined using the combination of PNA lectin histochemistry for the acrosomes of spermatids and Hoechst staining for chromatin in the nuclei, according to the established criteria for defining stages based on the position, size, and shape of acrosomes [18, 19].

The slides were mounted using ProLong Diamond Antifade Mountant (P36961; Thermo-Fisher Scientific, Kyoto, Japan) prior to microscopic examination. To quantify the proportion of RB2-positive germ cells in the seminiferous tubules, 200 seminiferous tubule sections were observed in two tissue sections obtained from two discrete portions of a testis from a single mouse. We evaluated the two tissue sections per mouse ($n = 6$ per group) using a microscope (BX51; Olympus Co., Tokyo, Japan) equipped with cellSens imaging software (Olympus Co., Tokyo, Japan).

2.4. Isolation of Spermatozoa from the Caput or Cauda Epididymis and RB2 Staining. For isolation of spermatozoa, the caput or cauda epididymis from each animal was cut using a surgical blade and then minced into small pieces, using scissors, in 10 mM HEPES-buffered TYH culture medium (119 mM NaCl, 4.8 mM KCl, 1.7 mM CaCl$_2$, 1.2 mM KH$_2$PO$_4$, 1.2 mM MgSO$_4$, 25 mM NaHCO$_3$, 5.6 mM glucose, 1.0 mM sodium pyruvate, and 4 mg/mL bovine serum albumin; pH 7.4). A small sample of the sperm suspension from the caput or cauda epididymis was spread onto a glass slide using a centrifugal autosmear technique (Cyto-Tek; Sakura, Tokyo, Japan). The spermatozoa were then fixed with methanol for 5 min and stained with 0.1% RB2 in 100 mM carbonate–bicarbonate buffer (pH 10) for 30 min. The slides were rinsed with carbonate–bicarbonate buffer to remove any excess dye. They were then mounted using ProLong Diamond Antifade Mountant (P36961; Thermo-Fisher Scientific) prior to microscopic examination. We observed 200 spermatozoa per mouse ($n = 6$ per group) using the BX51 microscope (Olympus) equipped with cellSens imaging software.

2.5. Analysis of Spermatozoan Motility. For motility analysis, cauda spermatozoa were collected according to our previously reported method, with minor modifications [19, 20]. Briefly, the cauda epididymis was dissected, and the connective tissue, fat pad, muscles, and vas deferens were removed. For sampling of spermatozoa, the cauda epididymis from each animal was cut using a surgical blade and then minced, using small scissors, into 10 mM HEPES-buffered TYH culture medium, as described above. The spermatozoa in suspension were allowed to disperse and swim up for 15 min on a warming tray at 37°C. The suspension was then filtered through a 40-μm nylon filter (PP-40N; Kyoshin Rikoh, Tokyo, Japan) to remove any undigested tissue fragments, and cauda spermatozoa were collected to evaluate motility. The motile spermatozoa were incubated for 2 hr at 37°C to allow hyperactivation.

The percentage of motile or hyperactivated spermatozoa was measured on the 37°C heated stage of a constant-temperature unit (MP-10; Kitazato Supply Co., Shizuoka, Japan), according to a previously described method [20]. Sperm motility was recorded using a phase-contrast microscope (CX43; Olympus, Tokyo, Japan) with a Moticam 1080 (Shimadzu Rika Co., Tokyo, Japan). Using a 10x phase-contrast objective, each field was recorded for 30 s, and the numbers of total spermatozoa and motile and/or hyperactivated spermatozoa were manually counted in three random fields for each sample. The analyses were performed in a blinded manner. Motile spermatozoa that exhibited asymmetric and whiplash flagellar movements and a circular and/or octagonal swimming locus were defined as hyperactivated [20, 21]. The percentage of motile spermatozoa was calculated as the number of forward motile and submotile spermatozoa or hyperactivated spermatozoa/total number of spermatozoa $\times 100$ (%).

2.6. In Vitro RB2-Binding Assay. RB2 dye in 100 mM carbonate–bicarbonate buffer (pH 10) was mixed with human spermatozoa PRM (Briar Patch Biosciences, Livermore, CA, USA) or mouse synthetic PRM1 or PRM2 (Briar Patch Biosciences) on noncoated glass slides. After the reaction, the glass slides were mounted and observed under a microscope. As a negative control, bovine serum albumin (BSA; 23209; Pierce™ BSA standard ampules, 2 mg/mL; Thermo-Fisher Scientific, Waltham, MA, USA) and intracellular proteins extracted from the human HeLa cell line (from the Japanese Collection of Research Bioresources Cell Bank) were mixed with RB2 dye in 100 mM carbonate–bicarbonate buffer (pH 10) or 10 mM phosphate buffer saline (pH 7.2). HeLa cells were cultured in Dulbecco's modified Eagle's medium (D5030, Sigma-Aldrich) supplemented with 10% fetal bovine serum (10099, Thermo-Fisher Scientific) and 100 μg/mL kanamycin (420311, Sigma-Aldrich). The cells were lysed with sodium dodecyl sulfate (SDS) lysis buffer (100 mM Tris-HCl at pH 8, 10% glycerol, and 1% SDS) to extract the intracellular proteins.

2.7. Statistical Analysis. Data are presented as mean ± standard deviation (GraphPad Prism version 9, GraphPad Software Inc., San Diego, CA, USA). Welch's t-test was used to

detect significant differences between the control and busulfan-treated groups (GraphPad Prism version 9). Statistical significance was defined by $P < 0.05$.

3. Results

3.1. Body and Organ Weights.
Body weight did not differ significantly between the control and busulfan-treated mice (control: 25.3 ± 0.7 g, busulfan-treated: 24.9 ± 0.4 g). Images of the gross appearance of the testes and epididymis in both the control and busulfan-treated mice are shown in Figure S2 (a)–S2(d). The absolute weights of the testes (left: control = 104.6 ± 3.1 mg, busulfan-treated = 32.6 ± 2.7 mg, $P < 0.001$; right: control = 108.7 ± 7.8 mg; busulfan-treated = 31.5 ± 3.9 mg, $P < 0.001$) and the epididymis (left: control = 36.4 ± 3.3 mg, busulfan-treated = 25.3 ± 2.0 mg, $P < 0.001$; right: control = 36.6 ± 3.2 mg, busulfan-treated = 25.6 ± 2.2 mg, $P < 0.001$) were significantly lower in the busulfan-treated mice than in the control mice. In particular, the caput epididymis of busulfan-treated mice was significantly smaller than that of the control mice (Figure S2(d)).

3.2. RB2 Specifically Stains Male Haploid Germ Cells Expressing PRMs.
Based on the shape of the acrosomes of the round and elongating spermatids (steps 1–12), we determined the corresponding staging of the mouse seminiferous epithelium cycle (stages I–XII) (Figure S3). When we had identified the germ cell population by staging the mouse seminiferous epithelium cycle (Figures 1(a), 1(c), 1(e), 1(g), 1(i), 1(k), 1(m), 1(o), 1(q), 1(s), 1(u), and 1(w)), using adjacent testis sections from the control mice, RB2-positive cells were observed in steps 12–16 of elongating and elongated spermatids in stages XII and I–VIII, but not in stages IX–XI of the seminiferous epithelium cycle (Figures 1(b), 1(d), 1(f), 1(h), 1(j), 1(l), 1(n), 1(p), 1(r), 1(t), 1(v), and 1(x)).

Quantitative histological analysis showed that busulfan-treated mice had approximately twice as many seminiferous epithelium tubules as those in the control, with loss of steps 12–16 of elongating and elongated spermatids (Figure 2(a)–2(g)).

3.3. RB2 Staining to Evaluate Epididymal Sperm Toxicity.
The percentage of motile spermatozoa in busulfan-treated mice was significantly lower than that in control mice ($P < 0.01$) (Figure 3(a)). The percentage of hyperactivated spermatozoa in busulfan-treated mice also showed a significant decrease as compared with that in the control group ($P < 0.01$) (Figure 3(b)). Swim-up spermatozoa collected from the cauda epididymis of both control (Figure 3(c)) and busulfan-treated (Figure 3(d)) mice showed RB2 staining. Spermatozoa collected from the caput epididymis in control mice were also stained with RB2 (Figure 3(e)), whereas those of busulfan-treated mice showed no positive staining (Figure 3(f)).

RB2-positive germ cells were detected in the caput epididymis of the control mice (Figures 4(a), 4(c), 4(e), and 4(g)), but not in the caput epididymis of busulfan-treated mice (Figures 4(b), 4(d), and 4(f)), matching the observations of the spermatozoa collected from the caput epididymis (Figure 3(e)).

3.4. pH Dependence of RB2 Specificity for PRMs.
Aggregates were observed when RB2 (pH 10) was mixed with human spermatozoa PRMs as well as when it was mixed with mouse synthetic PRMs (Figure 5(a)–5(f)); however, no aggregates were detected in the mixture of RB2 with BSA or with the intracellular proteins extracted from HeLa cells (Figure 5(g)–5(i)). In addition, this PRM-specificity of RB2 was lost at neutral pH, as the histones of somatic cells were stained (Figure 5(j)).

4. Discussion

Histopathology of the testes is the best nonclinical endpoint for the evaluation of testicular toxicity. A better understanding of spermatogenesis is necessary to identify and interpret the effects of chemicals on testis histology. If a drug candidate compound affects male germ cell development, it should not be considered further for drug development. However, the results of nonclinical animal testing may not necessarily align with the effects found in humans [2, 3]. An ideal evaluation system for nonclinical toxicological studies of drug development should allow accurate and easy determination of testicular toxicity. However, no staining technique is currently available for identifying male germ cell development, specifically in cases of complicated histology.

Kaneko et al. [12] demonstrated that, at pH 10, RB2 specifically stained the nucleus of human spermatozoa, without staining other cellular components of the human seminal fluid, thus providing a new method to evaluate sperm quality. The present study further demonstrated that this RB2 staining technique is also applicable to other mammalian species, such as well-established rodent models used for the evaluation of testicular toxicity of drug candidates in preclinical studies. Thus, RB2 staining provides a novel method for visualizing the nuclei of male mouse haploid germ cells. As both human and rodent spermatogenic cells can be visualized by RB2 staining, it may be useful to extrapolate the effects of pharmaceuticals on the testes and epididymis of rodents to humans under conditions of time and resource constraints.

In mice, the 12 stages (stages I–XII) of spermatogenesis were determined using the combination of PNA lectin histochemistry for the acrosomes of spermatids and Hoechst staining for the chromatin in the nuclei, according to the established criteria of staging based on the position, size, and shape of acrosomes [18, 19]. We found that RB2 staining could only visualize steps 12–16 haploid elongating and elongated spermatids, but not spermatogonia, spermatocytes, and step 1–11 spermatids at pH 10. These findings matched those for human spermatozoa [12]. Primates and most rodents, as well as a subset of other placental mammals, express two PRMs: PRM1 and PRM2 [6]. Both corresponding genes are transcribed in round spermatids (steps 7–9 in mice) [22, 23], and the mRNAs are stored in the form of cytoplasmic ribonucleoprotein particles until they are translated in elongating and elongated spermatids (steps 12–16)
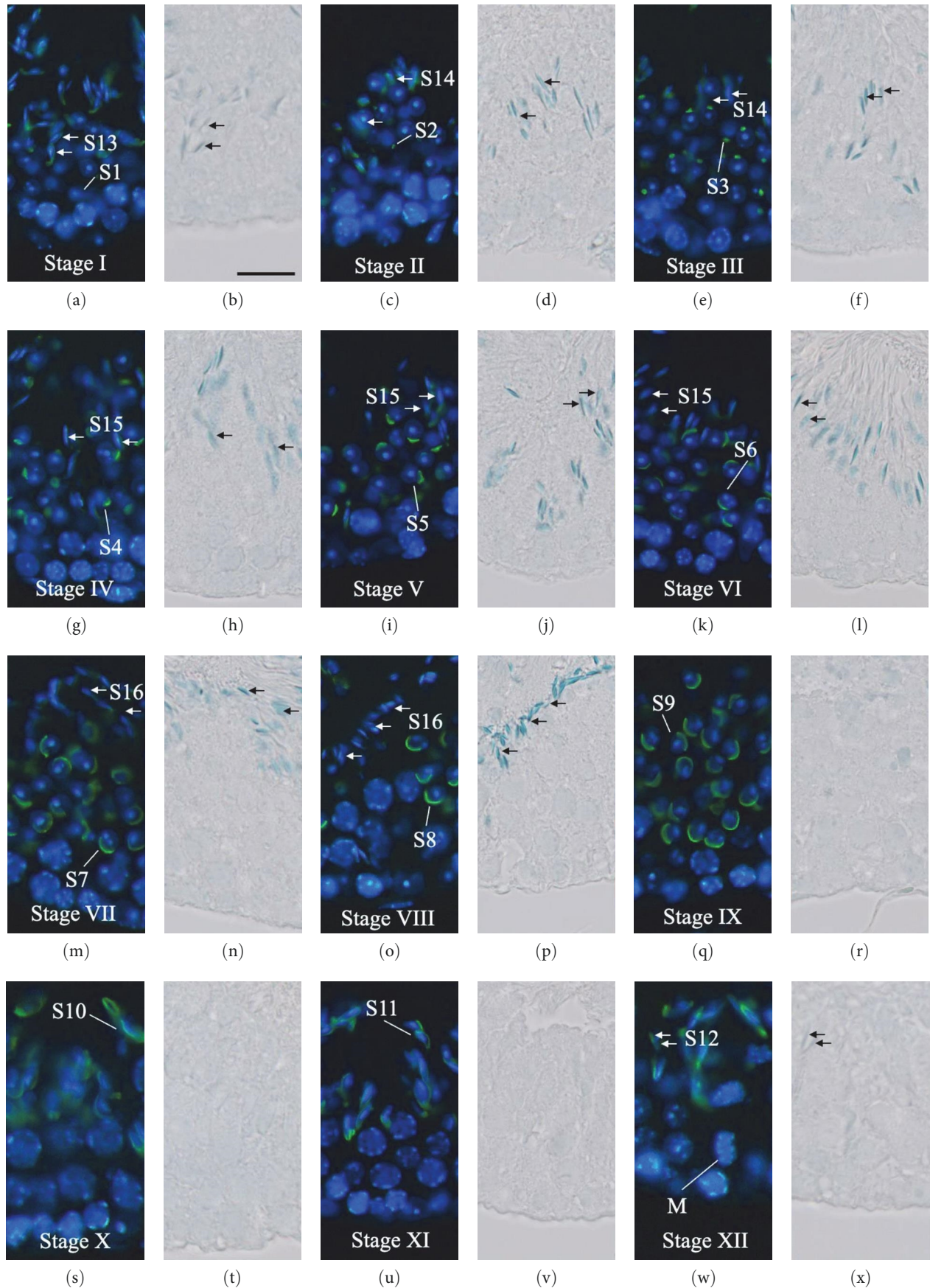
FIGURE 1: Distribution of reactive blue 2 (RB2)-positive male germ cells in the seminiferous tubules. (a, c, e, g, i, k, m, o, q, s, u, w) Determination of stages (I–XII) and identification of cell types. The nuclei of mouse control testis sections are stained with Hoechst 33258 (blue), and the acrosomes are stained with peanut agglutinin lectin histochemistry (green). (b, d, f, h, j, l, n, p, r, t, v, x) Haploid male germ cells are stained with RB2 dye. M, spermatocytes undergoing the first meiotic division; S1–16, steps 1–16 spermatids. White lines: S1–11. White arrows: S12–16. Black arrows: RB2-positive S12–16 spermatids. Scale bars: 20 μm.

(a)

(b)

(c)

(d)

(e)

(f)

(g)

FIGURE 2: Representative photographs of hematoxylin and eosin (H&E)- or reactive blue 2 (RB2)-stained testicular cross-sections from control and busulfan-treated mice. The incidence of RB2-positive spermatids in the seminiferous tubules was examined via light microscopy. (a) HE- or (d) RB2-stained sections from the testes of control mice. (b, c) HE- or (e, f) RB2-stained sections from the testes of busulfan-treated mice. Black arrows: RB2-positive spermatids. (g) Violin plot of the percentage of RB2-positive spermatids in the seminiferous tubules from control (200 tubules/section, $n = 6$) and busulfan-treated (200 tubules/section, $n = 6$) mice. Violin plots depict the frequency distribution of numerical data. Asterisks indicate significant differences between the control and busulfan-treated groups ($***P < 0.001$). Black arrows: RB2-positive spermatids. Scale bars: 20 μm.
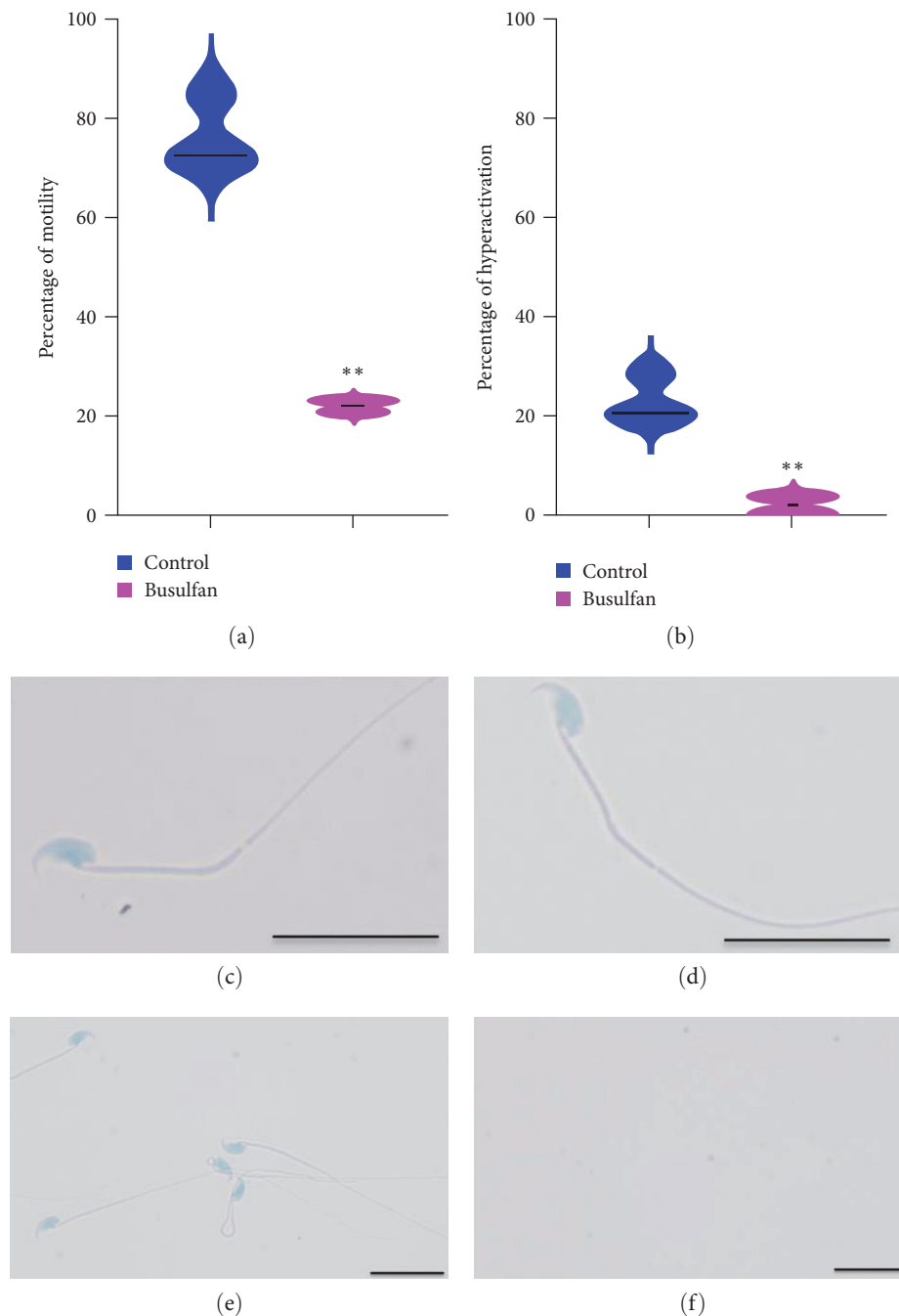
FIGURE 3: Sperm parameters in the control and busulfan-treated mice. Violin plots showing the percentage of (a) motile or (b) hyperactivated spermatozoa in the control ($n = 6$) and busulfan-treated ($n = 6$) mice. Reactive blue 2 (RB2)-stained spermatozoa from the cauda epididymis in the (c) control and (d) busulfan-treated mice. RB2 staining of spermatozoa from the caput epididymis in (e) control mice and (f) busulfan-treated mice. $^{**}P < 0.01$ vs. control.

[24, 25]. Following transcript storage, mouse *Prm1* mRNA seems to be translated earlier (step 12) than *Prm2* mRNA (steps 14 and 15) [26]. Therefore, our results suggest that RB2 specifically binds to PRMs expressed in steps 12–16 haploid spermatids in mouse seminiferous tubules [24–26].

Aggregates were detected in the mixture of RB2 dye (pH 10) with both human sperm PRM and mouse synthetic PRM reference standards, but not with BSA standard or intracellular proteins without PRMs extracted from somatic cells

(HeLa cells). These results suggest that a certain molecular component of PRMs can chemically interact with a component of RB2. We further explored the mechanism by which RB2 stains PRMs. We hypothesized that the unique binding specificity of RB2 to PRMs indicates an electrostatic ionic interaction. Lysine (Lys) and Arg are two positively charged amino acids that have high aqueous dissociation constants in proteins (ca. 10.5 for lysine (Lys) [27] and ca. 12.5 for Arg [28]), indicating a strong propensity for holding a positive
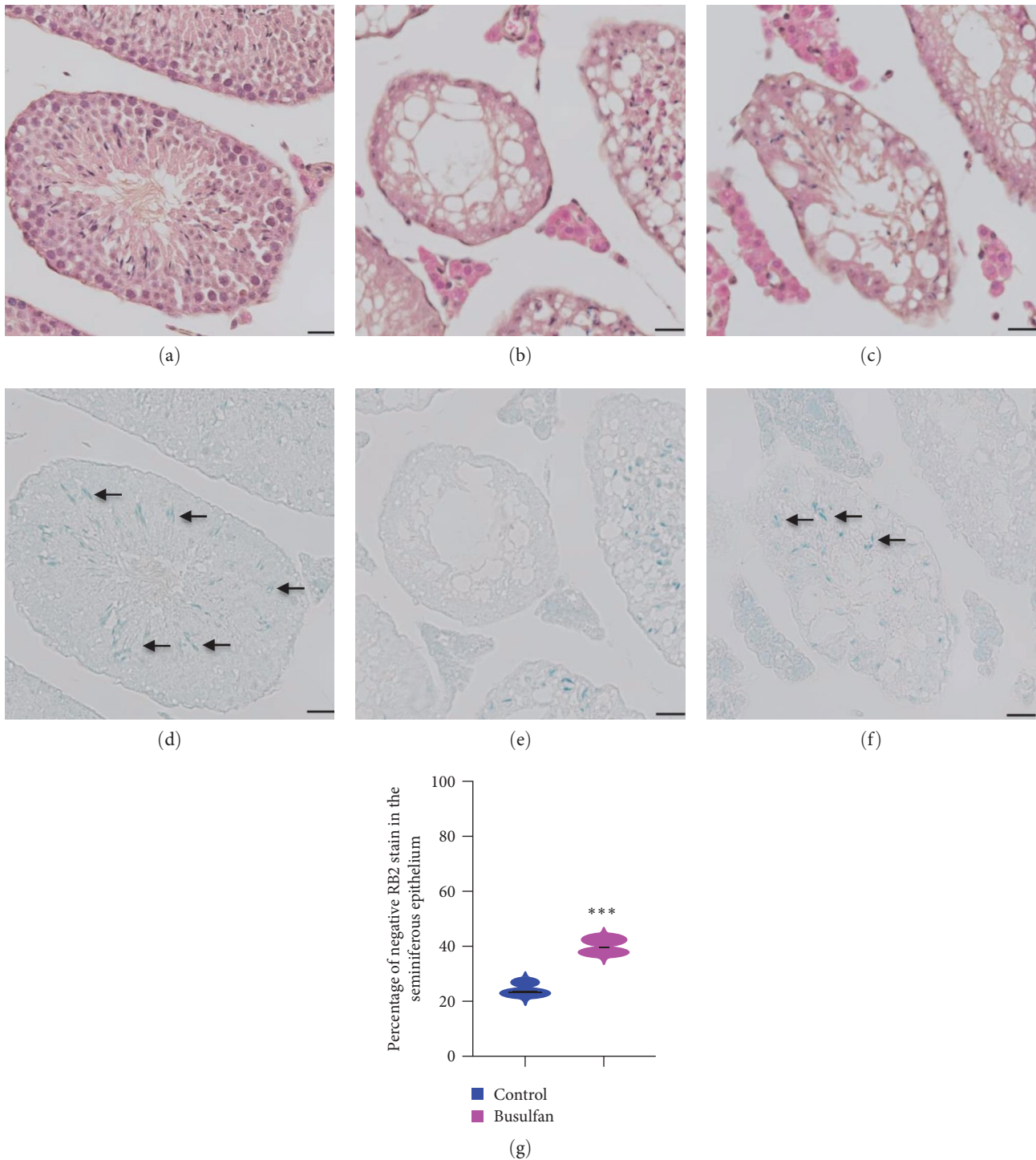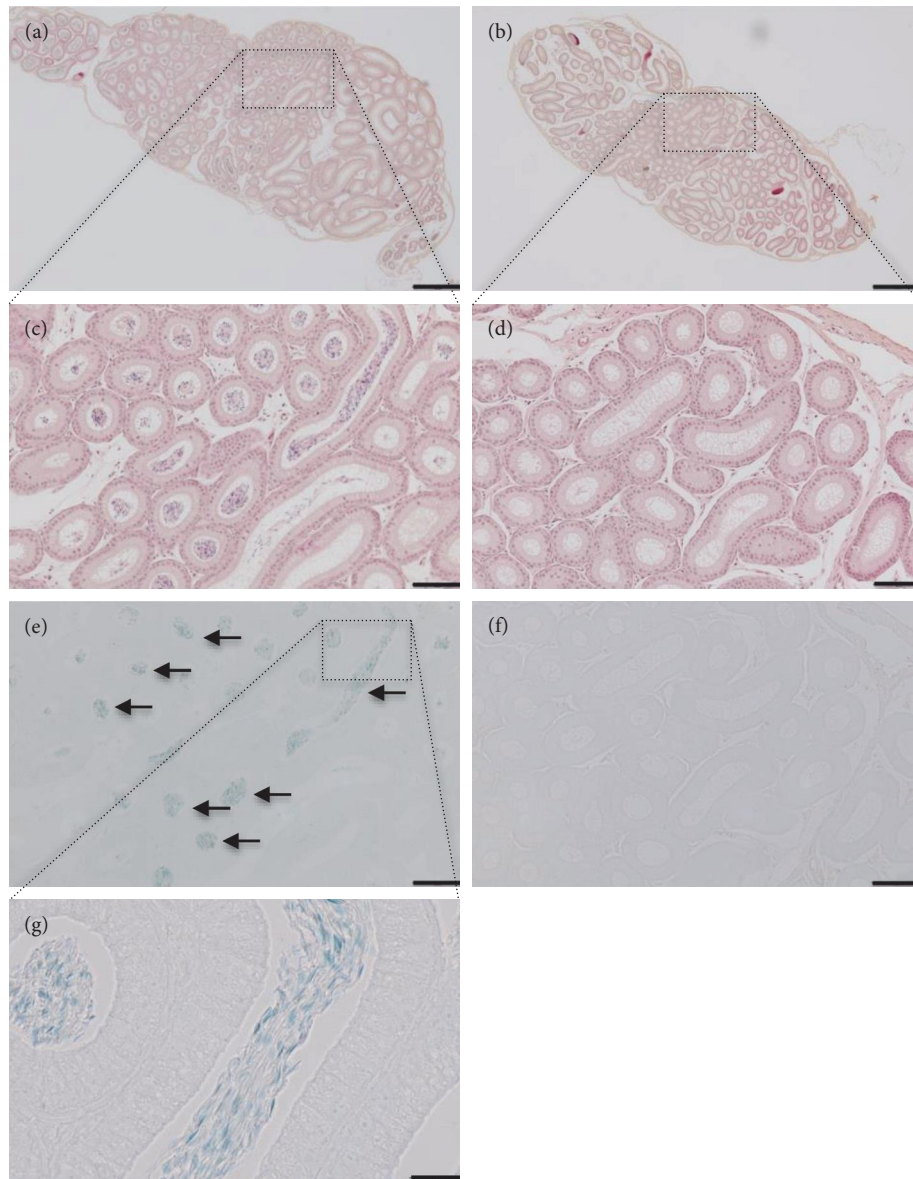
Figure 4: Representative photographs of hematoxylin and eosin (H&E)- and reactive blue 2 (RB2)-stained caput epididymal cross-sections from control and busulfan-treated mice. Low-magnification images of the morphology in the caput epididymis of (a) control and (b) busulfan-treated mice. High-magnification images of the morphology in the caput epididymis of (c) control and (d) busulfan-treated mice. (e) RB2-positive spermatozoa in the caput epididymis adjacent to the HE-stained section of control mice (c), with no RB2 staining (f) detected adjacent to the HE-stained section in the busulfan-treated group (d). (g) RB2-positive spermatozoa in the caput epididymis of control mice under the highest magnification (1,000x). Black arrows: RB2-positive spermatozoa. Scale bars: (a, b) 500 μm, (c–f) 100 μm, and (g) 20 μm.

charge at a neutral pH. In contrast, at pH > 10, Arg becomes positively charged, whereas Lys turns neutral [27, 28]. Therefore, the negative charge of the three sulfate residues in RB2 could ionically bind to the guanidyl group of Arg at pH 10 but not to the neutral chemical components of Lys. The present study demonstrated that RB2 specifically stained steps 12–16 spermatids, in which most PRMs are translated, at pH 10, as previously reported [24–26], whereas the specificity of RB2 staining was lost at a neutral pH when both Lys and Arg are positively charged. This pH-dependent specificity could be due to differences in the Arg content among the

basic proteins, histones, transition proteins, and PRMs. PRMs are typically short, basic proteins rich in positively charged Arg residues, allowing the formation of a highly condensed complex with the paternal genomic DNA, which has a strong negative charge [29–32]. The higher Arg content allows PRMs to form more stable complexes with DNA than would other basic proteins, such as histones and transition proteins [4]. Lys and Arg account for ∼20%–30% of the amino acids in histones, whereas Arg accounts for 70% of the amino acids in PRMs [4]. Thus, the higher content of Arg in the PRMs of steps 12–16 spermatids could explain the
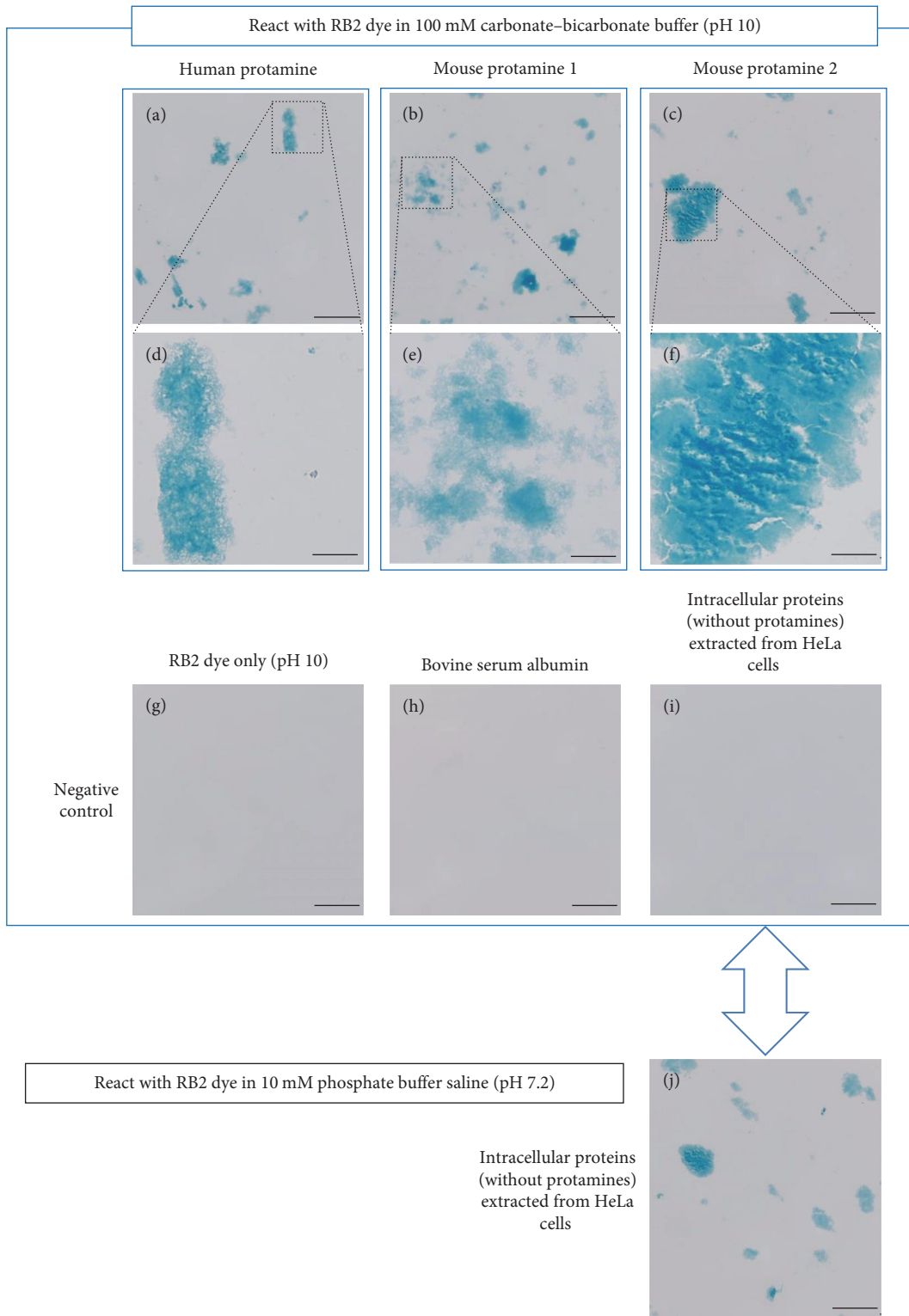
FIGURE 5: Representative photographs of the mixture of reactive blue 2 (RB2) dye and proteins. Aggregates detected in (a, d) human protamine, (b, e) mouse synthetic protamine 1, and (c, f) mouse synthetic protamine 2 standards. (g–i) No aggregates were detected in the RB2 dye-only sample (g), bovine serum albumin standard (h), and intracellular proteins (without protamines) extracted from HeLa cells (i). (j) However, at a neutral pH, the specificity of RB2 staining was lost in a mixture of RB2 dye and intracellular proteins (without protamines) extracted from HeLa cells. Scale bars: (a–c, g–i) 100 μm, (d–f) 20 μm.

FIGURE 6: Schematic illustration of reactive blue 2 (RB2)-positive haploid spermatids in the seminiferous tubules.

specificity of the novel RB2 staining technique under weakly alkaline conditions (pH 10).

Finally, with respect to the technical application of this method for male reproductive toxicity evaluation, we demonstrated that the percentage of RB2-positive spermatids in the seminiferous tubules of mice decreased after busulfan administration. In addition, no RB2-positive spermatozoa were detected in the caput epididymis of busulfan-treated mice, whereas spermatozoa of the cauda epididymis were stained with RB2 in both control and busulfan-treated mice. These results suggest that busulfan administration during spermiogenesis and sperm maturation decreases the abundance of PRMs, causing male infertility. Indeed, busulfan treatment significantly decreased the percentage of motile or hyperactivated spermatozoa, which is a common index of male fertility. These results suggested that the RB2 staining technique can facilitate rapid assessment of a drug's toxicity on male reproductive system, such as causing spermatogenic dysfunction and/or impairment of sperm maturation. This is achieved by simple visualization of the protamination of male haploid germ cells, which provides useful and supportive data to complement the results of conventional H&E staining.

The proposed RB2 staining method offers a more convenient tool for rapid visualization of PRMs than does immunohistochemical analysis using anti-PRM antibodies. This will be useful not only for the field of reproductive toxicology but also in general research in the fields of reproductive medicine and andrology, to improve the diagnosis of infertility in both humans and rodents.

Altered levels of PRMs may result in increased susceptibility to injury of the spermatozoal DNA, causing infertility or poor outcomes in assisted reproduction [33]. In general, mammalian reproduction relies on the successful transport of the paternal genome to the oocyte via motile spermatozoa, and the formation of functional spermatozoa requires a specific and well-orchestrated differentiation process in the testes [34]. PRMs may be important for remodeling of the chromatin complex following the elongation and condensation of the spermatogenic cell nucleus into a hydrodynamic shape [33, 35]. Paternal chromatin is completely remodeled from nucleohistones (nucleosomes) to nucleoprotamines during spermiogenesis to prepare for fertilization [6, 33]. In clinical studies, PRM deficiency was related to the exacerbation of sperm quality and DNA fragmentation [36]. Thus, using spermatozoa with abnormal PRM levels during assisted reproductive technology raises serious concerns for the developing embryo [37]. Therefore, altered PRM abundance in spermatozoa could serve as an important biomarker of male infertility. In this regard, using RB2 as a novel and PRM-specific

staining technique could enable rapid evaluation of protamination during spermiogenesis as supportive data for histopathological analysis.

Another major finding of the present study was that RB2 staining did not detect any spermatozoa in the caput epididymis within 28 days after busulfan administration (40 mg/kg body weight) to mice. Spermatogenesis is a complex process in which many spermatozoa are produced from a relatively small pool of spermatogonial stem cells [34]. To the best of our knowledge, most studies on busulfan have largely focused on testicular toxicity. As an alkylating agent, busulfan causes DNA damage by cross-linking DNA and was reported to kill A1 spermatogonia (a type of spermatogonial stem cell) specifically, as a side effect [38]. In mice, busulfan administered at 40 mg/kg body weight caused complete depletion of A1 spermatogonia up to the pachytene spermatocytes in stage VIII, within 12 days [39]. Since the proliferation and differentiation of A1 spermatogonia into elongated spermatids takes ~34.4 days in the testes [34], the spermatozoa in the caput epididymis were not likely triggered by damage to the A1 spermatogonia within 28 days of busulfan administration. In general, epididymal sperm toxicity evaluation may be more challenging than testicular toxicity evaluation. The epididymis is a single highly convoluted duct lined with a complex pseudostratified epithelium consisting of multiple cell types, including principal cells, basal cells, clear cells, apical cells, and halo cells [40]. The number and appearance of individual cell types also vary between the segments of the epididymis (i.e., initial segment, caput, corpus, and cauda). The present study demonstrated that RB2 is a specific dye for staining the spermatozoa and could therefore allow a higher throughput in epididymal toxicity evaluation.

5. Conclusion

In conclusion, we have demonstrated a novel methodology for visualizing male haploid germ cells using RB2 dye (see Figure 6), which represents a useful approach for evaluating the effects of pharmaceuticals, such as anticancer drugs, on testicular and epididymal toxicity. Nevertheless, this study had some limitations. The data obtained were insufficient for time-course evaluation. Spermatogenesis is a continuous, cyclical, and synchronized process that occurs in the epithelium of the seminiferous tubules of the testes, spanning ~34.4 days in mice and 74 days in humans [34]. In addition, sperm maturation requires ~10 days in both mice and humans [34]. Chemicals may affect the testes and epididymis at any time point throughout these cycles. Therefore, precisely predicting when and where testicular and epididymal toxicity may occur is difficult. This requires investigation at multiple time points to assess the potential recovery from drug toxicity, which is particularly important for anticancer drugs. Hence, further studies are needed to evaluate the time-course changes in PRM abundance in histological testis specimens and in the spermatozoa by utilizing the RB2 staining method.

Data Availability

The data used to support the findings of this study are included within the article.

Disclosure

This manuscript was submitted as a preprint in the link at https://www.biorxiv.org/content/10.1101/2023.03.06 .531276v2 [41].

Conflicts of Interest

The authors do not have any conflicts of interest to declare.

Authors' Contributions

SY conceived and designed the experiments. S Kitajima supervised this study. SY, TW, HM, KS, and MF performed the experiments. SY, TW, S Kaneko, and S Kitajima discussed the data analysis results. SY drafted the manuscript. All authors critically revised the article for intellectual content and approved the final version for publication.

Supplementary Materials

Figure S1: representative images for reactive blue 2 obtained from Pubchem (https://pubchem.ncbi.nlm.nih.gov). Figure S2: gross appearance of the testes and epididymis in control and busulfan-treated mice. Figure S3: determination of stages I–XII in the mouse seminiferous tubules. (*Supplementary Materials*)

References

[1] L. L. Lanning, D. M. Creasy, R. E. Chapin et al., "Recommended approaches for the evaluation of testicular and epididymal toxicity," *Toxicologic Pathology*, vol. 30, no. 4, pp. 507–520, 2002.

[2] A. R. Scialli, R. V. Clark, and R. E. Chapin, "Predictivity of nonclinical male reproductive findings for human effects," *Birth Defects Research*, vol. 110, no. 1, pp. 17–26, 2018.

[3] E. R. Rayburn, L. Gao, J. Ding, H. Ding, J. Shao, and H. Li, "FDA-approved drugs that are spermatotoxic in animals and the utility of animal testing for human risk prediction," *Journal of Assisted Reproduction and Genetics*, vol. 35, no. 2, pp. 191–212, 2018.

[4] R. Balhorn, "The protamine family of sperm nuclear proteins," *Genome Biology*, vol. 8, no. 9, Article ID 227, 2007.

[5] L. R. Brewer, M. Corzett, and R. Balhorn, "Protamine-induced condensation and decondensation of the same DNA molecule," *Science*, vol. 286, no. 5437, pp. 120–123, 1999.

[6] R. Oliva, "Protamines and male infertility," *Human Reproduction Update*, vol. 12, no. 4, pp. 417–435, 2006.

[7] C. Cho, H. Jung-Ha, W. D. Willis et al., "Protamine 2 deficiency leads to sperm DNA damage and embryo death in mice," *Biology of Reproduction*, vol. 69, no. 1, pp. 211–217, 2003.

[8] V. W. Aoki, L. Liu, and D. T. Carrell, "Identification and evaluation of a novel sperm protamine abnormality in a

population of infertile males," *Human Reproduction*, vol. 20, no. 5, pp. 1298–1306, 2005.

[9] D. T. Carrell, B. R. Emery, and S. Hammoud, "Altered protamine expression and diminished spermatogenesis: what is the link?" *Human Reproduction Update*, vol. 13, no. 3, pp. 313–327, 2007.

[10] C. Cho, W. D. Willis, E. H. Goulding et al., "Haploinsufficiency of protamine-1 or -2 causes infertility in mice," *Nature Genetics*, vol. 28, no. 1, pp. 82–86, 2001.

[11] I. A. Belokopytova, E. I. Kostyleva, A. N. Tomilin, and V. I. Vorob'ev, "Human male infertility may be due to a decrease of the protamine P2 content in sperm chromatin," *Molecular Reproduction and Development*, vol. 34, no. 1, pp. 53–57, 1993.

[12] S. Kaneko, J. Yoshida, and K. Takamatsu, "Low density regions of DNA in human sperm appear as vacuoles after translucent staining with reactive blue 2," *Journal of Medical Diagnostic Methods*, vol. 2, no. 6, pp. 1–5, 2013.

[13] Y. Xie, C.-C. Deng, B. Ouyang et al., "Establishing a nonlethal and efficient mouse model of male gonadotoxicity by intraperitoneal busulfan injection," *Asian Journal of Andrology*, vol. 22, no. 2, pp. 184–191, 2020.

[14] H. Nakata, T. Nakano, S. Iseki, and A. Mizokami, "Three-dimensional analysis of busulfan-induced spermatogenesis disorder in mice," *Frontiers in Cell and Developmental Biology*, vol. 8, Article ID 609278, 2020.

[15] K. Gutierrez, W. G. Glanzner, R. O. Chemeris et al., "Gonadotoxic effects of busulfan in two strains of mice," *Reproductive Toxicology*, vol. 59, pp. 31–39, 2016.

[16] D. Z. Wang, X. H. Zhou, Y. L. Yuan, and X. M. Zheng, "Optimal dose of busulfan for depleting testicular germ cells of recipient mice before spermatogonial transplantation," *Asian Journal of Andrology*, vol. 12, no. 2, pp. 263–270, 2010.

[17] S. Yokota, H. Miyaso, T. Hirai et al., "Development of a non-invasive method for testicular toxicity evaluation using a novel compact magnetic resonance imaging system," *The Journal of Toxicological Sciences*, vol. 48, no. 2, pp. 57–64, 2023.

[18] T. Wakayama, S. Yokota, K. Noguchi, T. Sugawara, K. Sonoda, and A. Wanta, "Quantitative evaluation of spermatogenesis by fluorescent histochemistry," *Histochemistry and Cell Biology*, vol. 157, no. 3, pp. 287–295, 2022.

[19] S. Yokota, N. Sekine, T. Wakayama, and S. Oshio, "Impact of chronic vitamin A excess on sperm morphogenesis in mice," *Andrology*, vol. 9, no. 5, pp. 1579–1592, 2021.

[20] M. Fujinoki, "Suppression of progesterone-enhanced hyperactivation in hamster spermatozoa by estrogen," *Reproduction (Cambridge, England)*, vol. 140, no. 3, pp. 453–464, 2010.

[21] H. Mohri, K. Inaba, S. Ishijima, and S. A. Baba, "Tubulin-dynein system in flagellar and ciliary movement," *Proceedings of the Japan Academy, Series B*, vol. 88, no. 8, pp. 397–415, 2012.

[22] N. B. Hecht, P. A. Bower, S. H. Waters, P. C. Yelick, and R. J. Distel, "Evidence for haploid expression of mouse testicular genes," *Experimental Cell Research*, vol. 164, no. 1, pp. 183–190, 1986.

[23] N. B. Hecht, K. C. Kleene, P. C. Yelick, P. A. Johnson, D. D. Pravtcheva, and F. H. Ruddle, "Mapping of haploid expressed genes: genes for both mouse protamines are located on chromosome 16," *Somatic Cell and Molecular Genetics*, vol. 12, no. 2, pp. 203–208, 1986.

[24] K. C. Kleene, R. J. Distel, and N. B. Hecht, "Translational regulation and deadenylation of a protamine mRNA during spermiogenesis in the mouse," *Developmental Biology*, vol. 105, no. 1, pp. 71–79, 1984.

[25] K. C. Kleene, "Poly(A) shortening accompanies the activation of translation of five mRNAs during spermiogenesis in the mouse," *Development (Cambridge, England)*, vol. 106, no. 2, pp. 367–373, 1989.

[26] E. S. Klaus, N. H. Gonzalez, M. Bergmann et al., "Murine and human spermatids are characterized by numerous, newly synthesized and differentially expressed transcription factors and bromodomain-containing proteins," *Biology of Reproduction*, vol. 95, no. 1, pp. 4–4, 2016.

[27] M. J. Harms, J. L. Schlessman, M. S. Chimenti, G. R. Sue, A. Damjanović, and B. García-Moreno, "A buried lysine that titrates with a normal pKa: role of conformational flexibility at the protein-water interface as a determinant of pKa values," *Protein Science*, vol. 17, no. 5, pp. 833–845, 2008.

[28] C. A. Fitch, G. Platzer, M. Okon, B. E. Garcia-Moreno, and L. P. McIntosh, "Arginine: its pK_a value revisited," *Protein Science*, vol. 24, no. 5, pp. 752–761, 2015.

[29] R. Oliva and G. H. Dixon, "Vertebrate protamine gene evolution I. Sequence alignments and gene structure," *Journal of Molecular Evolution*, vol. 30, no. 4, pp. 333–346, 1990.

[30] R. Oliva and G. H. Dixon, "Progress in nucleic acid research and molecular biology," *Progress in Nucleic Acid Research and Molecular Biology*, vol. 40, pp. 25–94, 1991.

[31] J. D. Retief, R. J. Winkfein, G. H. Dixon et al., "Evolution of protamine P1 genes in primates," *Journal of Molecular Evolution*, vol. 37, no. 4, pp. 426–434, 1993.

[32] L. Lüke, A. Vicens, M. Tourmente, and E. R. Roldan, "Evolution of protamine genes and changes in sperm head phenotype in rodents," *Biology of Reproduction*, vol. 90, no. 3, Article ID 67, 2014.

[33] D. Miller, M. Brinkworth, and D. Iles, "Paternal DNA packaging in spermatozoa: more than the sum of its parts? DNA, histones, protamines and epigenetics," *Reproduction (Cambridge, England)*, vol. 139, no. 2, pp. 287–301, 2010.

[34] A. P. Fayomi and K. E. Orwig, "Spermatogonial stem cells and spermatogenesis in mice, monkeys and men," *Stem Cell Research*, vol. 29, pp. 207–214, 2018.

[35] W. S. Ward, "Function of sperm chromatin structural elements in fertilization and development," *Molecular Human Reproduction*, vol. 16, no. 1, pp. 30–36, 2009.

[36] K. Ni, A.-N. Spiess, H.-C. Schuppe, and K. Steger, "The impact of sperm protamine deficiency and sperm DNA damage on human male fertility: a systematic review and meta-analysis," *Andrology*, vol. 4, no. 5, pp. 789–799, 2016.

[37] R. Dada, M. Kumar, R. Jesudasan, J. L. Fernández, J. Gosálvez, and A. Agarwal, "Epigenetics and its role in male infertility," *Journal of Assisted Reproduction and Genetics*, vol. 29, no. 3, pp. 213–223, 2012.

[38] L. R. Bucci and M. L. Meistrich, "Effects of busulfan on murine spermatogenesis: cytotoxicity, sterility, sperm abnormalities, and dominant lethal mutations," *Mutation Research*, vol. 176, no. 2, pp. 259–268, 1987.

[39] D. G. de Rooij and M. F. Kramer, "The effect of three alkylating agents on the seminiferous epithelium of rodents. I. Depletory effect," *Virchows Archiv B Cell Pathology*, vol. 4, no. 1, pp. 267–275, 1970.

[40] V. D. Rinaldi, E. Donnard, K. Gellatly et al., "An atlas of cell types in the mouse epididymis and vas deferens," *eLife*, vol. 9, Article ID 9, 2020.

[41] S. Yokota, T. Wakayama, H. Miyaso et al., "Reactive blue 2 labels protamine in late-haploid spermatids and spermatozoa and can be used for toxicity evaluation," *bioRxiv*, 2023.